Review Article

Chronic pulmonary embolism: diagnosis

Katia Hidemi Nishiyama[1], Sachin S. Saboo[2], Yuki Tanabe[2], Dany Jasinowodolinski[3], Michael J. Landay[2], Fernando Uliana Kay[2]

[1]Department of Thoracic Imaging, Hospital do Coração and DASA (Diagnósticos da América), São Paulo, Brazil; [2]Department of Radiology, UT Southwestern Medical Center, Florence Building, Dallas, TX, USA; [3]Department of Thoracic Imaging, Hospital do Coração, São Paulo, Brazil

Contributions: (I) Conception and design: KH Nishiyama, FU Kay; (II) Administrative support: FU Kay, D Jasinowodolinski; (III) Provision of study material or patients: All authors; (IV) Collection and assembly of data: All authors; (V) Data analysis and interpretation: All authors; (VI) Manuscript writing: All authors; (VII) Final approval of manuscript: All authors.

Correspondence to: Fernando Uliana Kay, MD, MBA. Department of Radiology, UT Southwestern Medical Center, Florence Building (E6.120), 5323 Harry Hines Boulevard, Dallas, TX 75390-9316, USA. Email: fernando.kay@utsouthwestern.edu.

Abstract: Chronic thromboembolic pulmonary hypertension (CTEPH) is a complication of venous thromboembolic disease. Differently from other causes of pulmonary hypertension, CTEPH is potentially curable with surgery (thromboendarterectomy) or balloon pulmonary angioplasty. Imaging plays a central role in CTEPH diagnosis. The combination of techniques such as lung scintigraphy, computed tomography and magnetic resonance angiography provides non-invasive anatomic and functional information. Conventional pulmonary angiography (CPA) with right heart catheterization (RHC) is considered the gold standard method for diagnosing CTEPH. In this review, we discuss the utility of these imaging techniques in the diagnosis of CTEPH.

Keywords: Pulmonary embolism; chronic; computed tomography; V/Q; pulmonary hypertension

Submitted Oct 28, 2017. Accepted for publication Jan 12, 2018.
doi: 10.21037/cdt.2018.01.09
View this article at: http://dx.doi.org/10.21037/cdt.2018.01.09

Introduction

Deep vein thrombosis and pulmonary embolism (PE) are major health issues which affect up to 600,000 patients per year in the U.S. (1). Most patients will fully recover after an episode of PE, with resolution of the emboli and restoration of blood flow (2,3). However, in a small subset of patients, residual clots will remain attached to pulmonary vessels walls, leading to organization and fibrosis, resulting in blood flow impairment and increased pulmonary vascular resistance (4). In addition to these events, endothelial dysfunction and small vessel remodeling may also play a role in the genesis of pulmonary hypertension (5). The current World Health Organization classification on pulmonary hypertension considers chronic thromboembolic pulmonary hypertension (CTEPH) as a separate group (group 4) given to its distinctive pathophysiology (6).

A literature review identified epidemiological data on CTEPH available by June 2014 in the U.S., Europe and Japan (7). In the U.S. and Europe, the crude annual incidence of CTEPH was 3–5 cases per 100,000 individuals/year. The incidence of CTEPH in U.S. and Europe following an episode of PE ranged from 0.1% to 9.1% (7). A recent meta-analysis revealed pooled CTEPH incidence of 0.56% in all consecutive patients with symptomatic PE (3). A large prospective single-center study found respective PAH incidences of 1%, 3%, and 4% at 6, 12, and 24 months following a PE episode, despite anticoagulation therapy (2). This study revealed that a previous pulmonary embolism, younger age, a larger perfusion defect, and idiopathic pulmonary embolism at presentation increased the risk of CTEPH (2). Given the long latency from the embolic episode to symptom onset (average time-interval of 18 months), CTEPH may be frequently under-recognized, and patients will present with severe functional limitation by the time of diagnosis (8). It is known that CTEPH prognosis heavily depends on hemodynamic severity, notably in those without therapeutic intervention. A 30%

3-year survival has been reported in patients with a mean pulmonary artery pressure (mPAP) higher than 30 mmHg (9). The study reported respective mortality rates of 12% and 50% for patients with mPAP <30 mmHg [mild pulmonary arterial hypertension (PAH)] and mPAP >30 mmHg, thus highlighting initial use of anticoagulation for patients with proximal CTEPH and mild PAH, reserving endarterectomy for failure of medical therapy (9).

Despite its poor prognosis, CTEPH is a potentially curable disease (10). Pulmonary endarterectomy is the treatment of choice in CTEPH patients, with declining mortality rates as low as 2.2% in experienced centers (11). Pulmonary thromboendarterectomy removes obstructive and hardened thrombus and markedly improves the hemodynamic measures of mean pulmonary-artery pressure, pulmonary vascular resistance, and cardiac output. Improvement in hemodynamics causes reverse right ventricular remodeling and the return of right ventricular systolic and diastolic function toward normal levels (12-15). Balloon pulmonary angioplasty is an emerging treatment modality for inoperable patients (16-20), currently limited to experienced and high-volume CTEPH centers (10).

CTEPH diagnosis

PAH is a term reserved for patients with pre-capillary pulmonary hypertension. The diagnostic criteria for PAH includes a resting mean pulmonary arterial pressure greater than or equal to 25 mmHg and pulmonary arterial wedge pressure less than or equal to 15 mmHg on right heart catheterization (RHC). PAH caused by thromboembolic disease is suggested by segmental perfusion defects without matching ventilation abnormalities on ventilation/perfusion lung scintigraphy (V/Q scan). Further presence of specific imaging findings on computed tomography pulmonary angiography (CTPA), cardiovascular magnetic resonance (CMR) imaging or conventional pulmonary angiography (CPA) will define the diagnosis of CTEPH (10). The diagnostic criteria for CTEPH are summarized in *Figure 1*.

Multiple risk factors have been linked to CTEPH, such as underlying autoimmune or hematological disorders (e.g., lupus anticoagulant or antiphospholipid syndrome), cancer and other comorbidities such as ventriculoatrial shunts, infected pacemaker leads, splenectomy, non-O blood group, and thyroid replacement therapy (21-23). Potential etiologies have been attributed to increased hypercoagulability, reduced fibrinolytic capacity, and genetic polymorphisms leading to fibrinolysis resistance (24). Impaired angiogenesis and inflammation also seems to play an important role in the development of CTEPH; however, there is no effective method to predict which patients with acute PE are at higher risk of developing CTEPH (25).

CTEPH symptoms are nonspecific and usually related to the development of pulmonary hypertension. Patients may be asymptomatic for several years before presenting with progressive exertional dyspnea, chronic nonproductive cough, atypical chest pain, tachycardia, syncope and cor pulmonale. The clinical deterioration is usually related to loss of right ventricular functional capacity (26,27). The 6-minute walking test is commonly used and inexpensive method capable of providing prognostic information in patients with CTEPH (28,29).

Echocardiography

Resting transthoracic echocardiography is an imaging tool recommended for further assessment of suspected pulmonary hypertension (ACR appropriateness criteria rating: 9; where 1, 2, and 3 are usually not appropriate, 4, 5, 6 may be appropriate, and 7, 8, 9 are usually appropriate) (30). Although transthoracic echocardiography with Doppler imaging is sensitive for the detection of pulmonary hypertension and right ventricular dysfunction, it is not specific for the diagnosis of CTEPH, since it does not differentiate acute/subacute from chronic PE (31). Notwithstanding, it can exclude intracardiac shunts or left-sided heart disease as cause of pulmonary hypertension. Common echocardiography findings in CTEPH include right atrial and ventricular dilatation, right ventricular hypertrophy and hypokinesis, paradoxical deviation of the ventricular septum towards the left and tricuspid regurgitation. Pulsed Doppler assessment of the tricuspid regurgitant jet velocity provides an estimate of the pulmonary artery systolic pressure, which in turn can be used to estimate the mean pulmonary artery pressure (32).

RHC

RHC is a complementary method to echocardiography, usually indicated for further confirmation of the mean pulmonary artery pressure (ACR appropriateness criteria rating: 9) (30), especially when the diagnosis remains uncertain following non-invasive studies (10).

Other imaging modalities also have important roles in CTEPH management. The combination of different methods can provide detailed anatomic and functional

information, which may be used to further differentiate CTEPH from other causes of pulmonary hypertension, to aid in treatment planning, and to assess therapy response. The most common imaging methods used for those purposes are chest radiography (CXR), V/Q scan, conventional and dual-energy CTPA, CMR, and CPA.

CXR

CXR is often performed as part of the initial evaluation (ACR appropriateness criteria rating: 9) (30) and may be normal in the early stage of the disease. In advanced cases, CXR shows signs of pulmonary hypertension, such as dilatation of central pulmonary arteries (*Figure 2A*), enlargement of the cardiac silhouette and obliteration of the retrosternal clear space on the lateral view (*Figure 2B*). Right atrial enlargement on frontal CXR may also be observed. Other findings include lobar or segmental lung oligemia and pleuroparenchymal scarring secondary to previous embolic episodes (33,34). A study on 36 patients showed that the presence of an avascular pulmonary region or enlargement of the right interlobar pulmonary artery greater than 20 mm with pleural abnormality on CXR had respective sensitivity and specificity of 78% and 92% for differentiating CTEPH from primary pulmonary hypertension (35).

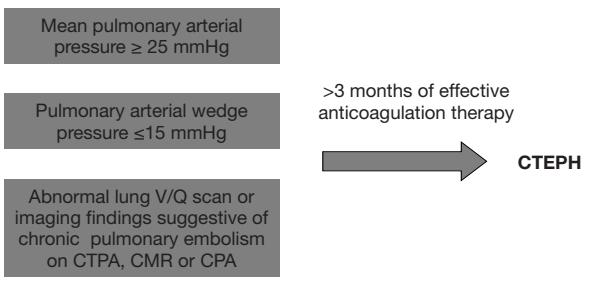

Figure 1 Diagnostic criteria for chronic thromboembolic pulmonary hypertension. CTEPH, chronic thromboembolic pulmonary hypertension; lung V/Q scan, ventilation/perfusion lung scintigraphy; CTPA, computed tomography pulmonary angiography; CMR, cardiovascular magnetic resonance; CPA, conventional pulmonary angiography.

Ventilation/perfusion lung scintigraphy

If on the one hand CTPA is the standard of care for diagnosing acute PE, on the other, V/Q scan is first-line screening modality for detecting CTEPH (ACR appropriateness criteria rating: 8) (10,30). In a retrospective study, V/Q scan has shown superiority to CTPA for diagnosing CTEPH, with respective sensitivities of 97% versus 51% and specificities of 90–95% *vs.* 99% (36). By contrast, a more recent prospective study revealed comparable accuracies between both methods in the diagnosis of CTEPH (37).

Diagnostic criteria for CTEPH on V/Q scans include

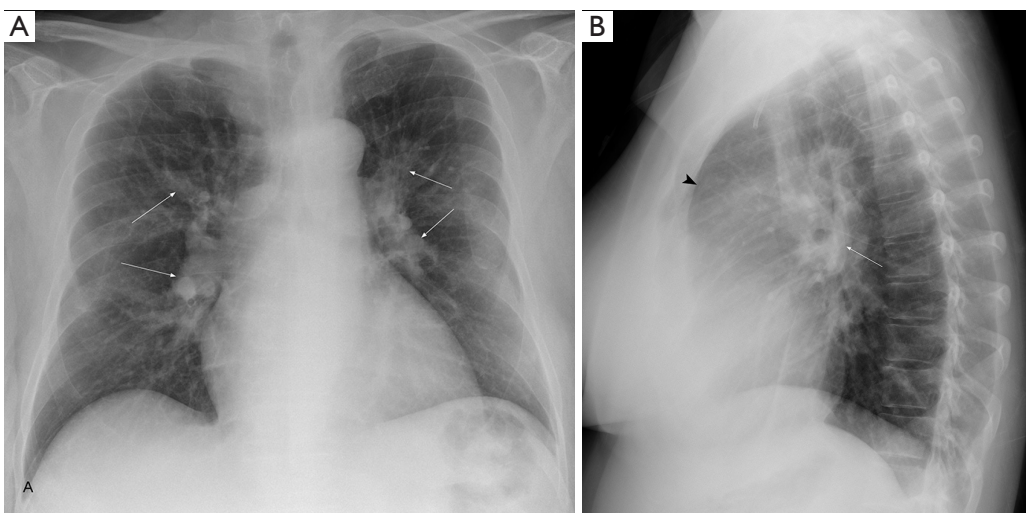

Figure 2 Frontal (A) and lateral (B) view chest radiographs show enlarged central pulmonary arteries (arrows), increased cardiothoracic index and obliteration of the retrosternal clear space (arrowhead).

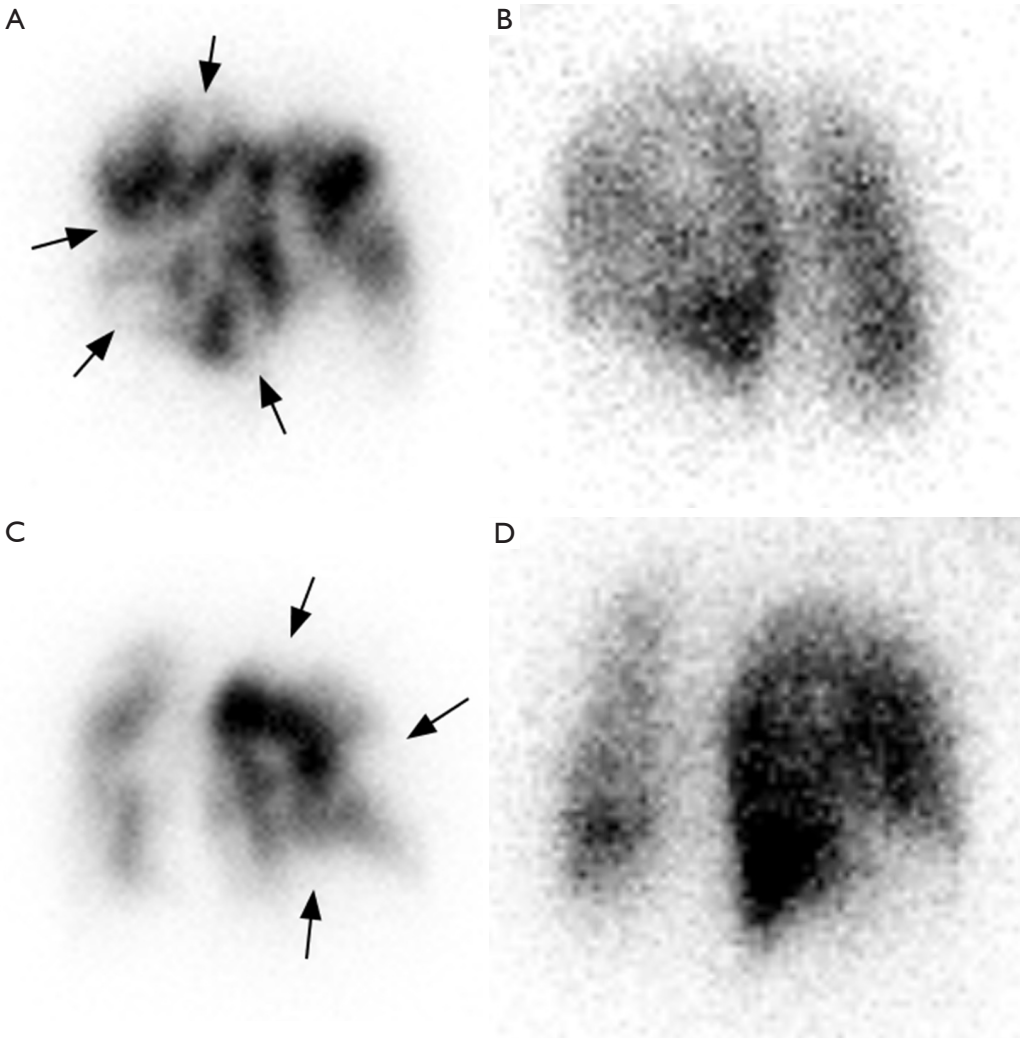

Figure 3 Left posterior oblique (LPO) imaging with intravenous injection of albumin macroaggregate-^{99m}Tc revealing multiple segmental perfusion defects in the left lung (arrows, A), with corresponding normal ventilation on LPO imaging obtained with inhalation of ^{133}Xenon (B). Right posterior oblique (RPO) perfusion scintigraphy also revealing mismatched segmental perfusion defects in the right lung (arrows, C) with normal ventilation (D).

one or more segmental or larger mismatched perfusion defects (*Figure 3*). *Table 1* summarizes the diagnosis criteria for pulmonary embolism on V/Q scans. Other causes of pulmonary hypertension (e.g., idiopathic PAH and pulmonary venoocclusive disease) generally present with normal scans or unmatched/non-segmental perfusion abnormalities (i.e., "mottled" perfusion scans) secondary to diffuse involvement of small-caliber vessels (38,39). It has been claimed that in addition to high diagnostic performance, V/Q scans could also deliver less radiation dose than CTPA (40); however, systematic comparisons with current dose-reduced CTPA protocols are lacking. Undisputedly, V/Q scans are a safer choice than CTPA in patients with severe iodine contrast allergy and with decreased renal function.

Normal findings at V/Q scans practically exclude the presence of chronic pulmonary thromboembolism; however, false negative results may be seen due to recanalization of chronic thrombi. False interpretation can also occur in areas of matched V/Q defects that reflect compensatory response of the lung chronic hypoperfusion, leading to reduction in ventilation. Another well-known pitfall of planar V/Q is

Table 1 Ventilation/perfusion scan interpretation criteria for pulmonary embolism

Category	Modified PIOPED II criteria
High likelihood ratio	≥2 large mismatched (ventilation-perfusion) segmental defects
Non-diagnostic	All other findings
Very low likelihood ratio	Non-segmental Q defect < chest radiograph lesion;
	1–3 segmental defects;
	Solitary matched (ventilation-perfusion: chest radiograph) defect (≤ 1 segment) in mid or upper lung;
	Stripe sign (peripheral perfusion in a defect);
	Solitary large pleural effusion (at least one third of pleural cavity);
	≥2 matched (ventilation-perfusion) defects, regionally normal chest radiograph
Normal	No Q defects

Q, perfusion. Reference: Sostman HD, Miniati M, Gottschalk A, *et al.* Sensitivity and specificity of perfusion scintigraphy combined with chest radiography for acute pulmonary embolism in PIOPED II. *J Nucl Med* 2008;49:1741-8.

"shine-though", which occurs when normally perfused areas overly hypoperfused areas on planar imaging, resulting in underestimation of the presence and extent of PE (41-43).

High-probability and non-diagnostic scans require further diagnostic workup since V/Q scans are not specific for CTEPH. Pathologies such as pulmonary artery sarcoma, fibrosing mediastinitis, vasculitis and extrinsic compression of pulmonary vasculature may also produce large segmental perfusion defects. In addition, V/Q scans do not allow determination of the magnitude, location or proximal extent of disease, and thus cannot predict its surgical operability (44). By contrast, single photon emission computed tomography (SPECT) V/Q can improve the accuracy for detecting and quantifying perfusion defects over planar V/Q scan and CTPA (45-48). SPECT-CT V/Q imaging may provide some anatomic information to help addressing non-embolic causes of perfusions defects (49), but with higher radiation dose due to adding a non-contrast CT acquisition.

CTPA

The role of CTPA in the diagnosis of acute PE has been robustly established (50). However, its importance in CTEPH diagnosis has been changing over time. Recent evidence suggests that the diagnostic performance of CTPA in CTEPH is non-inferior to that of V/Q scan (37). Studies have shown high sensitivity and specificity of CTPA for detecting chronic thromboembolic disease at the lobar (97–100% and 95–100% respectively) and segmental (86–100% and 93–99%) levels (51-53). Nevertheless, a negative CTPA does not exclude CTEPH, especially in cases where disease is confined to subsegmental level.

Radiation dose has been historically proposed as one of the shortcomings of CTPA, but recent evidence suggests significant decrease in effective doses in the last decade. The average effective radiation dose of CTPA was previously estimated in 15 mSv (with values between 13–40 mSv), in comparison with 2.0 mSv for lung perfusion ^{99m}Tc-MAA and 0.2 mSv for lung ventilation ^{99m}Tc-DTPA scans (54,55). Newer protocols utilizing tube current modulation and iterative reconstruction algorithms have allowed current effective doses of 7 mSv (56-58). One study has even proposed a submillisievert dose CTPA protocol for diagnosing pulmonary embolism (59) (6).

Imaging findings of pulmonary embolism vary according to the amount of vascular obstruction and to the degree of PAH. According to the location, radiologic findings may be subdivided into vascular and lung parenchymal features (*Table 2*).

Vascular features

Main features of CTEPH on CTPA include occlusive or non-occlusive filling defects in the pulmonary arteries (60,61). Vessel cutoff, abrupt decrease in vessel diameter and absence of contrast enhancement distal to the obstruction are features suggestive of occlusive CTEPH (*Figure 4*). Partial occlusive filling defects are usually seen as webs or bands of non-resolved thrombi after partial recanalization (62) (*Figure 5*). Organizing thrombi may

Table 2 CT pulmonary angiography imaging findings in chronic thromboembolic pulmonary hypertension

Chronic thromboembolic pulmonary hypertension signs	CTPA imaging findings
Vascular signs	Complete occlusion—vessel cutoff;
	Partial occlusion—webs, bands, focal stenotic vessel segment and areas of post-stenotic dilatation, irregular thickening of the vessel wall and reduced caliber, calcified residual thrombus, peripheral crescent-shaped defect
Collateral vessels	Bronchial artery dilation (> 2 mm) and tortuosity;
	Non-bronchial arteries: pleural, intercostal, phrenic, internal mammary
PH signs	Main pulmonary artery dilation (> 33 mm);
	Ratio main pulmonary artery diameter to ascending aorta diameter >1.1:1;
	Right ventricle enlargement and hypertrophy;
	Ratio right ventricle diameter to left ventricle diameter >1:1;
	Bowing of the interventricular septum toward the left ventricle;
	Right ventricular hypertrabeculation/hypertrophy
Lung parenchymal signs	Scars from prior pulmonary infarctions: bands, irregular peripheral linear opacities, wedge-shaped opacities with pleural thickening;
	Mosaic lung attenuation

CTPA, computed tomography pulmonary angiography; PH, pulmonary hypertension.

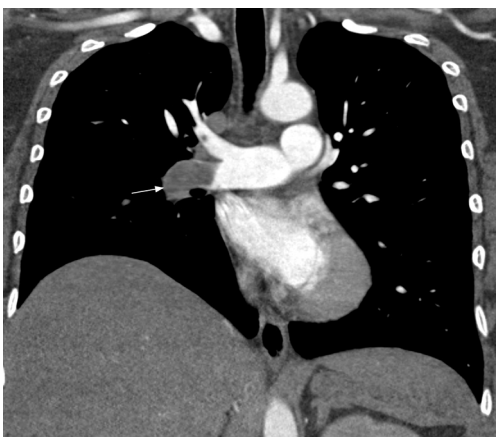

Figure 4 Coronal CT pulmonary angiography image shows a larger thrombus in the right interlobar artery with complete occlusion and vessel cutoff (arrow).

also cause focal stenotic arterial segments followed by post stenotic dilation. In more advanced cases, eccentric and irregular arterial wall thickening with reduced caliber are seen, secondary to contraction of the organizing thrombus (*Figure 6A,B*).

Chronic obstruction of the pulmonary arteries will lead to compensatory enlargement of the bronchial arteries; however, this is a non-specific finding encountered in many other conditions of reduced pulmonary artery flow, such as fibrotic interstitial lung disease, bronchiectasis, and chronic infection. Systemic collateralization may include pleural, intercostal, phrenic, and internal mammary arteries, and will depend of the degree of pulmonary hypoperfusion (*Figure 6B,C*). Dilation of the proximal segment of the bronchial arteries (greater than 2 mm in diameter) and tortuosity are findings not only indicative of collateral flow, but have also been described as predictors of survival after pulmonary thromboendarterectomy (63). Another study has shown that abnormally enlarged bronchial and non-bronchial arteries are more frequently found in CTEPH (73%) than in idiopathic PAH (14%) (64).

The increase in the pulmonary circulation resistance leads to higher pulmonary artery pressures, which will result in ancillary imaging findings. An absolute main pulmonary artery (MPA) diameter >29 mm (measured on the axial plane, at the bifurcation level and orthogonal to the long vessel axis) or an MPA-to-aorta diameter ratio >1:1 are predictors of pulmonary hypertension (65,66). To increase specificity, absolute MPA diameter ≥33 mm and MPA-to-aorta ratio >1.1:1 should be used for pulmonary

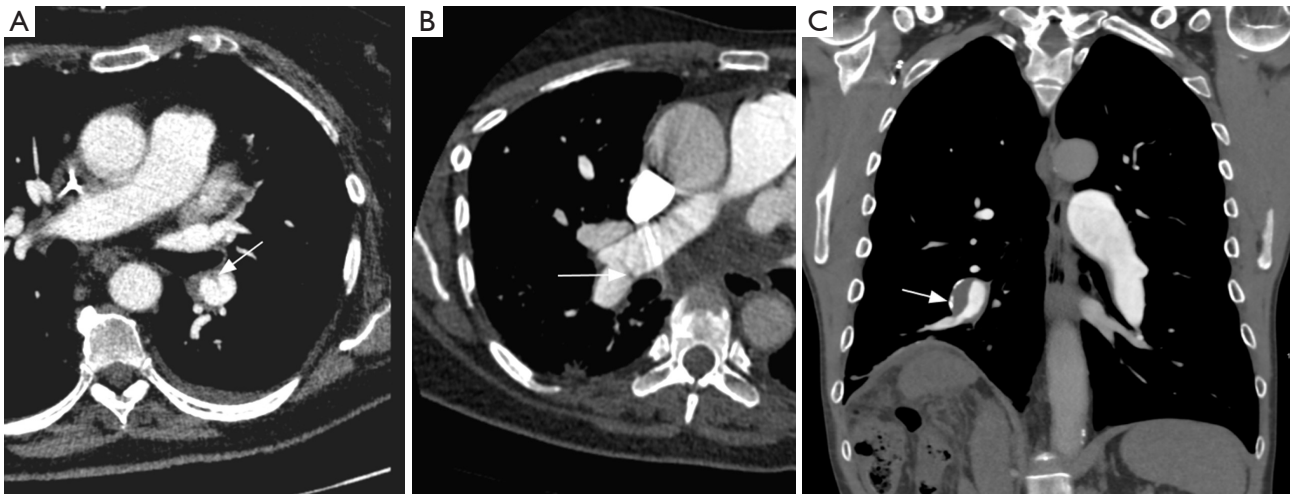

Figure 5 CT pulmonary angiography appearances of chronic thrombi in different patients. Axial images (A) and (B) show webs (arrows), reflecting non-resolved thrombi and partial recanalization. Coronal image (C) shows an eccentric thrombus in right interlobar pulmonary artery with calcified mural thickening (arrow).

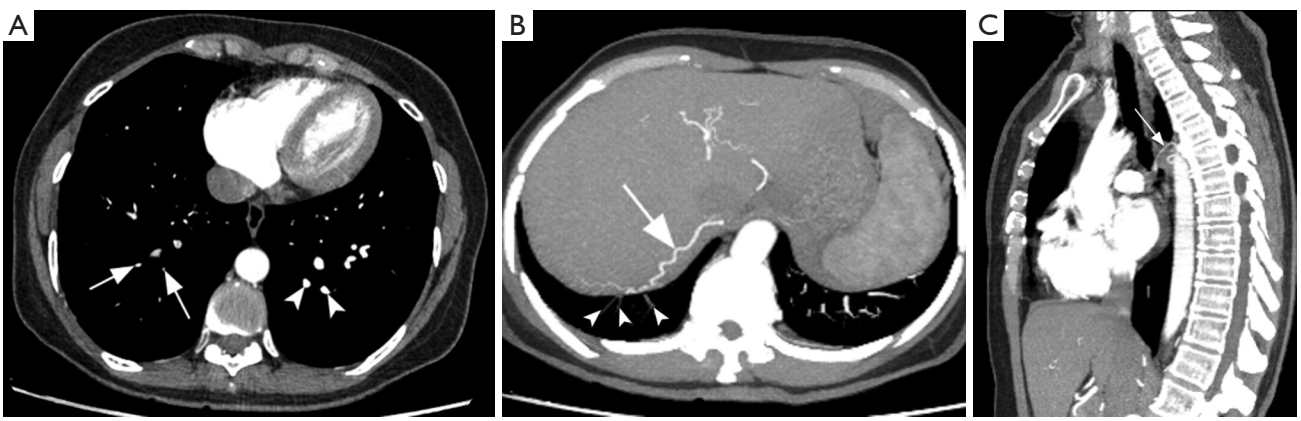

Figure 6 CT pulmonary angiography features of chronic thromboembolic pulmonary hypertension. Axial image (A) showing reduced caliber vessels (arrows) related to the contraction of the organizing thrombus and poor contrast opacification in comparison with contralateral arteries (arrowheads). Axial maximum intensity projection (MIP) at the thoracoabdominal transition (B) showing a prominent phrenic artery (arrow) providing systemic collateral circulation, in addition to asymmetric caliber of the pulmonary arteries in the lower lobes (attenuated on the right side, arrowheads). Sagittal MIP reconstruction (C) reveals a prominent bronchial artery providing systemic collateral circulation (arrow).

hypertension diagnosis (*Figure* 7) (67). Contrary to non-thrombotic causes of pulmonary hypertension, CTEPH usually present with asymmetric dilation of the pulmonary artery branches (60).

Over time, increased right-heart afterload will result in ventricular enlargement and hypertrophy. Accurate measurements of the cardiac chambers on CT relay on ECG-gating, which is not usually employed in CTPA. In a non-gated CTPA, a gross estimate of right-ventricular enlargement may be obtained by dividing the largest transverse diameter of the right by the left ventricle on the axial plane, with abnormal values greater than 1:1 (68-70). Bowing of the interventricular septum towards the left ventricle is another feature suggestive of right-heart strain (71).

Lung parenchyma features

Scars from prior pulmonary infarction may present with parenchymal bands, peripheral irregular linear, or wedge-

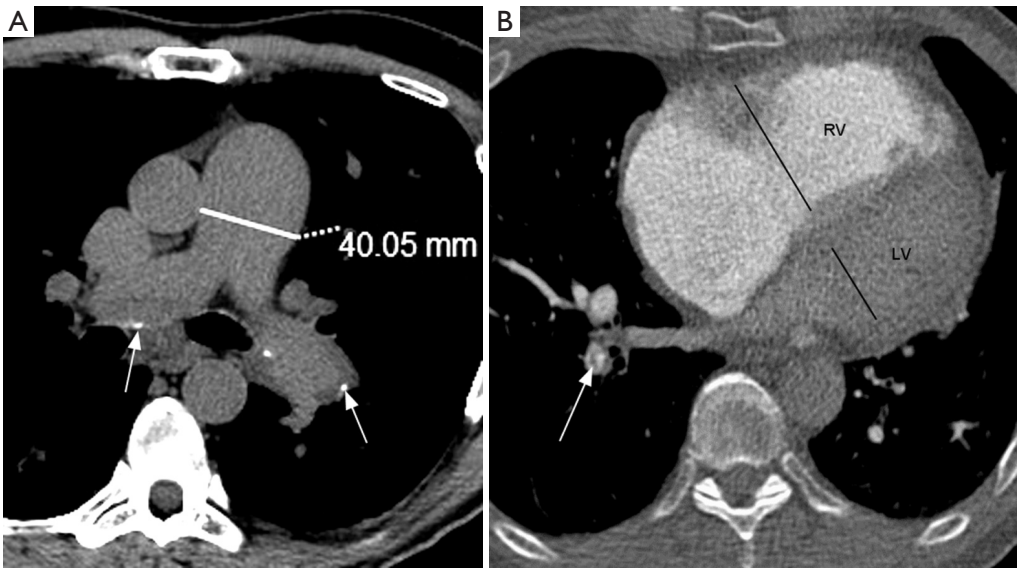

Figure 7 CT evaluation of pulmonary hypertension. (A) Noncontrast axial CT shows main pulmonary artery (MPA) of 40 mm and MPA/aorta ratio > 1.1:1, consistent with pulmonary hypertension. The absence of contrast facilitates the observation of chronic eccentric thrombi with mural calcification (arrows). Axial CT pulmonary angiography image (B) shows right ventricular enlargement (right-to-left ventricular ratio greater than 1:1). Webs noted in right lower lobe arteries, consistent with chronic pulmonary embolism (arrow).

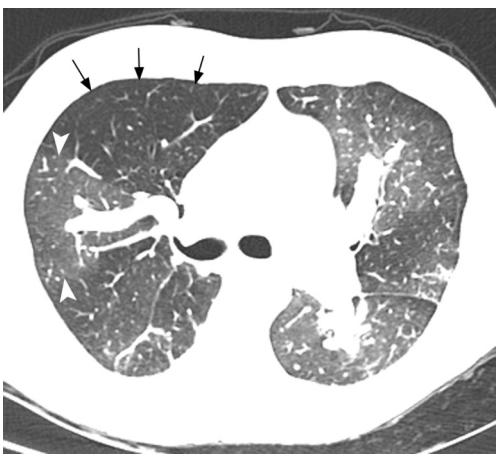

Figure 8 Regions of increased (arrowheads) and decreased lung attenuation (arrows) characterize lung mosaicism. Markedly reduced diameter of segmental/subsegmental arteries noted within areas of decreased lung attenuation.

shaped opacities. These changes are most commonly seen in the lower lobes, often accompanied by pleural thickening. Mosaic perfusion is another feature seen in CTEPH, characterized by alternating regions of increased and decreased lung attenuation due to heterogeneous perfusion (72,73). Marked variation in segmental arteries diameters is usually observed, thus aiding in the differentiation from ground glass opacities. In mosaic perfusion, decreased attenuation is secondary to hypoperfusion distal to the occluded/suboccluded arteries, whereas increased attenuation is related to redistribution of blood flow to patent vessels. In areas of increased attenuation, larger vessels and stronger enhancement after contrast material administration can be seen (60,61,74) (*Figure 8*). Although more commonly seen in patients with CTEPH, mosaic lung attenuation is nonspecific, and may be also seen in patients with PH due to cardiac or lung disease (75). Air trapping secondary to small airway disease can cause hypoxic vasoconstriction, also leading to mosaic perfusion on CT, usually associated with other features of bronchial disease (76). Interestingly, PE can also cause small airway obstruction/air trapping on exhalation images (77).

CPA

CPA has been considered the gold standard method for diagnosing CTEPH, providing confirmation of culprit lesions and evaluation of surgical accessibility. The set of imaging findings of chronic PE on CPA include pouch defects, vascular webs/bands, intimal irregularities (*Figure 9*), abrupt vascular narrowing, vascular obstructions

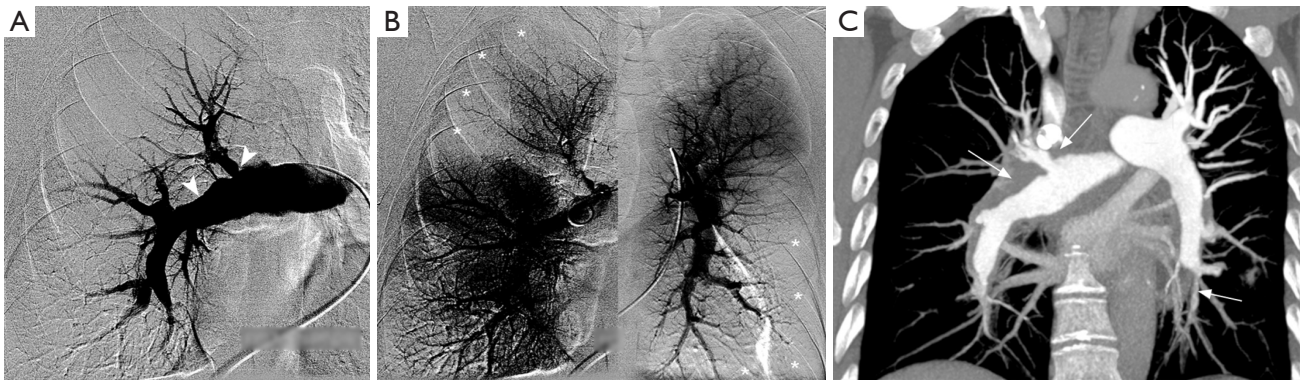

Figure 9 Conventional pulmonary angiography correlated with CT pulmonary angiography (CTPA). Selective right pulmonary angiography (A) showing irregularities at the origin of the right upper lobar and proximal interlobar pulmonary arteries (arrows in A), suggestive of chronic pulmonary embolism. Composite image of right and left pulmonary angiography (B) during parenchymal enhancement shows multiple hypoperfused areas, especially in right upper and left lower lobes (asterisks). Coronal maximum intensity projection CTPA (C) shows arterial wall thickening and luminal narrowing in the right pulmonary artery and segmental branches of the left lower lobar pulmonary artery (arrows).

and post-obstructive dilatations (78), and these findings are observed in proximal pulmonary artery in 63% of patients with CTEPH (79). Regarding diagnostic performance, Ley *et al.* indicated in a prospective study that the sensitivity of conventional angiography was 66% at the main/lobar level and 76% at the segmental level, both of which were lower than that of CTPA (51). The diagnostic role of CPA has been shifting towards conventional and dual-energy CTPA because of its invasiveness and dependency on interventional operator skills. However, CPA is usually performed in combination with RHC, which is indispensable for assessing pulmonary arterial hemodynamics (80). In addition, it may also be used for therapeutic intervention such as balloon pulmonary angioplasty (BPA), which is a treatment option for inoperable CTEPH (16).

Dual-energy computed tomography (DECT)

DECT estimates the density of materials, including iodine, based on their specific X-ray attenuation signatures at two energy levels (81). Iodine density and perfused blood volume (PBV, i.e., iodine in the lungs normalized by pulmonary artery density) can be used to evaluate lung perfusion. Several studies have shown substantial correlation between lung iodine density and perfusion, with comparable results to V/Q scans (82-85). To date, DECT role in thoracic imaging has mainly targeted at pulmonary embolic disease and PAH (61,86-88).

Perfusion defects in CTEPH are depicted as wedge-shaped areas of decreased iodine density on DECT, similarly to those seen in V/Q scans (*Figure 10*). However, careful interpretation is required when interpreting segmental perfusion defects on DECT. False-positive causes include beam hardening (e.g., a defect affecting the medial right upper pulmonary lung due to contrast in superior vena cava) and motion artifacts (e.g., near the heart or diaphragm) (89). Underlying lung parenchyma disease, such as bullous emphysema, is also cause of pseudo-defects (90). By contrast, perfusion defects can be missed (i.e., false negative) in areas of lung distal to affected vessel due to collateralization or sub-occlusive thrombus (91). Unlike ^{99m}TC-macroaggregated albumin in perfusion scanning, iodine is capable of entering collateral vessels. Despite limitations, one study has shown sensitivity of 96% and specificity of 76% of DECT in detecting perfusion defects (92) while another study showed sensitivity and specificity of 100% and 92% respectively in the diagnosis of CTEPH (93).

Recent studies have explored the correlation of PBV maps with severity of pulmonary arterial obstruction (91) and hemodynamic parameters. Meinel *et al.* showed that automated quantification of PBV was correlated with both systolic and mean pulmonary arterial pressure, but failed to find correlation between PBV and cardiac index or 6-minute walking distance (94). By contrast, Takagi *et al.* found that whole lung PBV score was not only associated with pulmonary arterial pressure, but also with pulmonary vascular resistance. Increased iodine density in

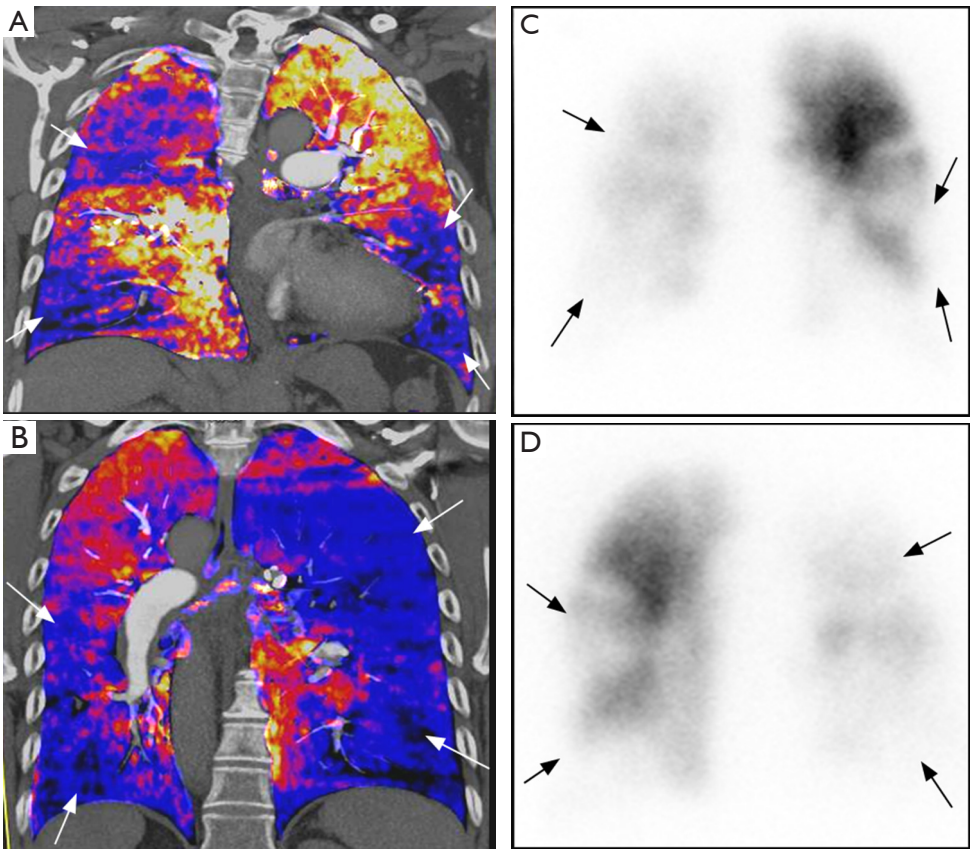

Figure 10 Dual-energy CT with V/Q scan correlation. (A,B) Coronal perfused blood volume map shows multiple segmental and lobar perfusion defects (blue areas, arrows). Planar anterior (C) and posterior (D) perfusion scintigraphy shows corresponding perfusion defects with similar distribution.

the pulmonary artery with simultaneously decrease in the whole lung iodine density has been found as a feature of increased pulmonary vascular resistance in PH (95). As with CTPA, need for intravenous iodinated contrast medium and exposure to ionizing radiation are shortcomings of this technique.

CMR angiography

Magnetic resonance imaging (MRI) allows not only assessment of the pulmonary arterial circulation with no radiation exposure, but also evaluation of pulmonary perfusion and hemodynamic impact on cardiac function. Magnetic resonance pulmonary angiography (MRPA) uses a three-dimensional T1-weighted gradient echo sequence with paramagnetic intravenous contrast material (gadolinium-based agents) to depict the pulmonary arterial bed, capable of identifying typical angiographic findings of CTEPH such as intraluminal webs/bands and abrupt vessel narrowing (*Figure 11*) (96). The diagnostic performance of MRPA for CTEPH diagnosis is similar to that of CPA, but still inferior to CTPA (10,51,96). On the other hand, 3-dimensional contrast-enhanced lung perfusion MRI has high diagnostic performance for diagnosing CTEPH. Rajaram *et al.* indicated that lung perfusion MRI has sensitivity of 97%, specificity 92%, positive predictive value 95% and negative predictive value 96% for detecting CTEPH, with comparable performance to perfusion scintigraphy and CTPA (97). Moreover, MRI allows accurate and reproducible functional assessment of the right ventricle when combined with cine techniques. Cardiac findings associated with CTEPH are right ventricular dysfunction and hypertrophy, paradoxical interventricular septal wall motion, and enlargement of pulmonary artery (98) (*Figure 12*). Despite its usefulness as one-stop shop modality for preoperative assessment

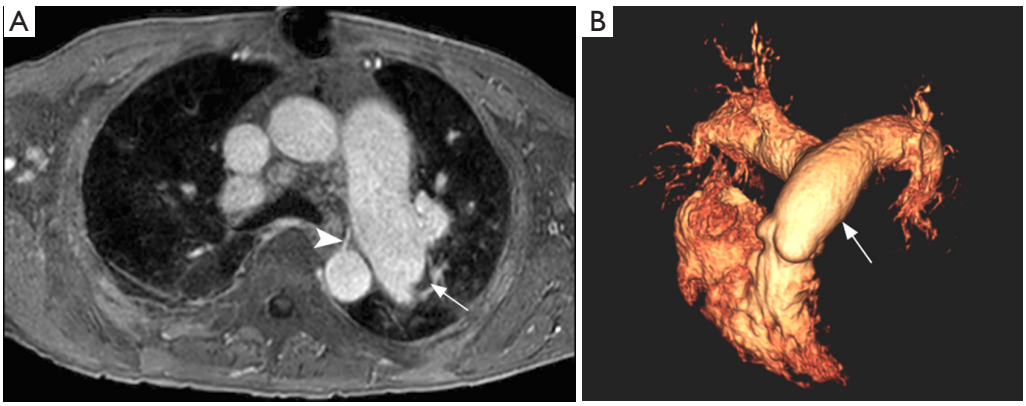

Figure 11 Magnetic resonance pulmonary angiography (MRPA). Axial post contrast fat-suppressed spoiled gradient recalled echo (A) shows left pulmonary artery dilation with a subtle eccentric crescent-shaped thrombus (arrow). Note a prominent bronchial artery arising from the descending aorta (arrowhead). Tridimensional volume rendered reconstruction (B) showing dilation of the main pulmonary artery (arrowhead) and central branches.

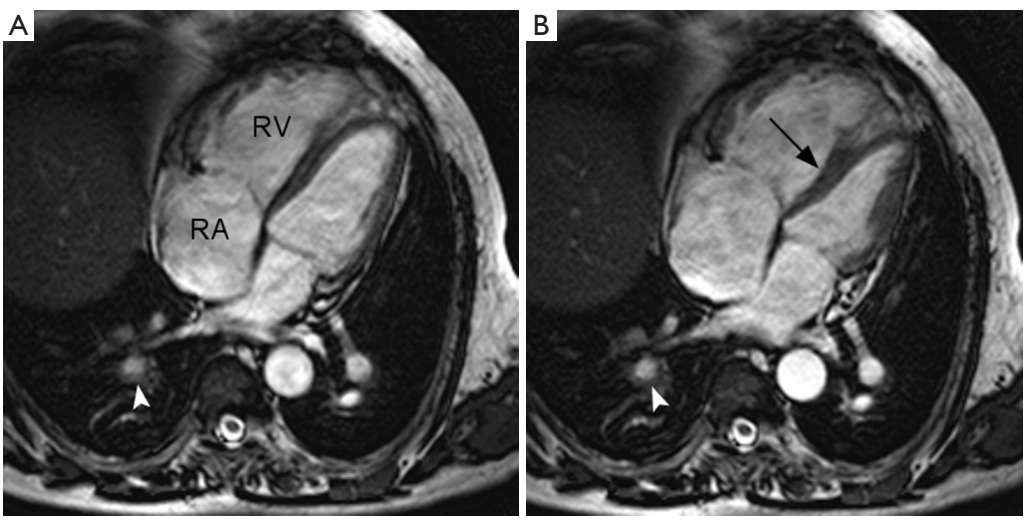

Figure 12 Cine balanced steady-state free precession imaging. Four-chamber view in end-diastole (A) and end-systole (B) showing dilation of the right atrium (RA) and ventricle (RV). Note paradoxical deviation of the interventricular septum towards the left (arrow) during systole. Pulmonary artery wall thickening and luminal narrowing is also seen in the right lower lobe (arrowheads), consistent with sequelae of chronic thromboembolic pulmonary hypertension (CTEPH).

of pulmonary artery and heart in CTEPH, MRI is still underutilized in this setting. A longer scan time and the association with nephrogenic systemic fibrosis (NSF) are some of the disadvantages of this method. NSF is a rare and potentially fatal fibrosing disease, and its association with gadolinium-based contrast agent (GBCA) exposure is widely accepted (99). The use of group I GBCA (gadodiamide, gadopentetate dimeglumine, and gadoversetamide) is contraindicated in patients considered at risk of developing NSF: those on dialysis of any form, severe or end-stage chronic kidney disease (CKD 4 or 5, i.e., estimated glomerular filtration rate <30 mL/min/1.73 m^2) without dialysis, and with acute kidney injury (100). The use of GBCA for MRI may also be associated with gadolinium retention in the brain; however, no evidence that this retention may be harmful has been proven to date (101,102).

Table 3 summarizes the advantages and disadvantages of different imaging modalities in CTEPH diagnosis.

Table 3 Imaging techniques, advantages and disadvantages in chronic thromboembolic pulmonary hypertension diagnosis

Imaging technique	Accuracy	Advantages	Disadvantages
Chest radiography	Low accuracy, may be normal in early stages	Good for initial evaluation; wide available	Need for further complementary investigation
Echocardiogram	Sensitive for PH detection however not specific for CTEPH	Exclusion of intracardiac shunt or left heart disease as a cause of PH	Need for further complementary investigation
Lung scintigraphy	High sensitivity and negative predictive value	Less radiation, more cost effective	Not specific for CTEPH, does not allow determination of exact location and extent of disease
CTPA	High accuracy	Wide available, rapid scan time, high spatial resolution, better evaluation of lung parenchyma	Radiation dose, need for iodinated intravenous contrast and complications related to it
DECT	Good accuracy	Perfusion map comparable to lung scintigraphy	Same as CTPA; newer technique—not available
CMR	Good accuracy; 3D contrast-enhanced lung perfusion: high accuracy	No radiation exposure; functional assessment of right ventricle	Relatively longer scan time relatively lower spatial resolution; lung parenchyma evaluation is limited
CPA with RHC	Gold standard	Determine location, extent and magnitude of disease and also predict its surgical operability	Invasive procedure

CTEPH, chronic pulmonary thromboembolism hypertension; CTPA, computed tomography pulmonary angiography; DECT, dual-energy computed tomography; CMR, cardiovascular magnetic resonance; CPA with RHC, conventional pulmonary angiography with right heart catheterization; PH, pulmonary hypertension.

Differential diagnosis of chronic pulmonary embolism

Some disorders involving the pulmonary artery tree can radiologically mimic chronic PE including congenital interruption, vasculitides, primary sarcoma, idiopathic pulmonary hypertension, acute thromboembolism, tumor thrombus/emboli and *in situ* thrombosis.

Acute pulmonary embolism

Chronic PE is often discovered during CTPA to evaluate acute PE, and sometimes acute and chronic embolism coexists. In acute occlusive PE, the diameter of the pulmonary artery is increased due to impaction of thrombus and pulsatile flow, while in chronic PE, the vessel distal to the obstruction is attenuated (103). Partial filling defects in acute PE may be central or eccentric, with an acute angle with vessel wall generally observed. Conversely, in partially occlusive chronic PE, a peripheral crescent-shaped defect presenting an obtuse angle with vessel wall is seen (*Figures 13*,*14*). Luminal narrowing, intimal irregularities, bands, webs and calcifications are other signs that may help to distinguish chronic from acute embolism (104,105). In addition, acute embolic obstruction may increase pulmonary vascular resistance and lead to acute pulmonary hypertension. However, right ventricular hypertrophy would require a latency time to develop. Presence of dilated bronchial arteries also suggests recurrent or chronic PE disease. While in acute PE, normal lung parenchyma or pulmonary infarction (non-enhancing opacity with bubbly lucencies or "reversed halo sign") are most commonly found, in chronic PE mosaic lung attenuation and lung parenchymal scars from prior infarction are hallmarks. *Table 4* summarizes main features used to differential chronic from acute pulmonary embolism on CTPA.

Proximal interruption of the pulmonary artery

Unilateral interruption of the pulmonary artery is a rare developmental anomaly that is commonly associated with other congenital cardiovascular disorders, such as Tetralogy of Fallot and septal defects. However, this condition may occur as an isolated finding in asymptomatic patients (106). Interruption of MPA tends to occur contralateral to the aortic arch, most commonly on the right side when unilateral. If associated with congenital heart disease, it is more commonly left-sided. The pulmonary artery ends

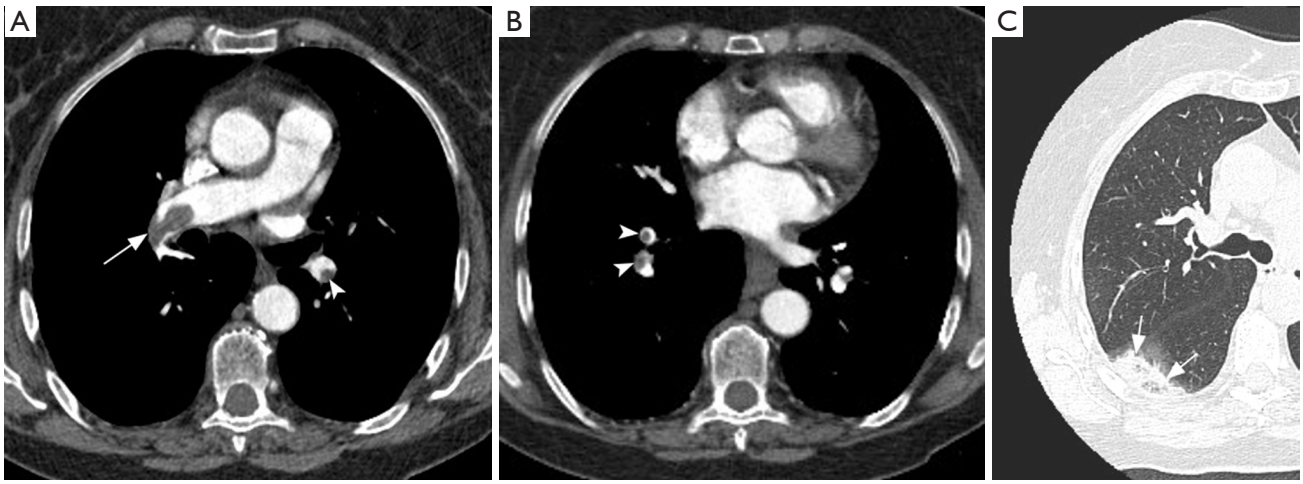

Figure 13 CT pulmonary angiography (CTPA) images in acute pulmonary embolism. Axial CTPA images (A and B) show partial filling defects, centrally located in the right pulmonary artery (arrow) and eccentric in segmental branches (arrowheads). Note acute angle between thrombi and vessel walls. Axial lung window (C) shows "reversed halo sign" in the right lower lobe (arrows), a nonspecific sign of pulmonary infarction.

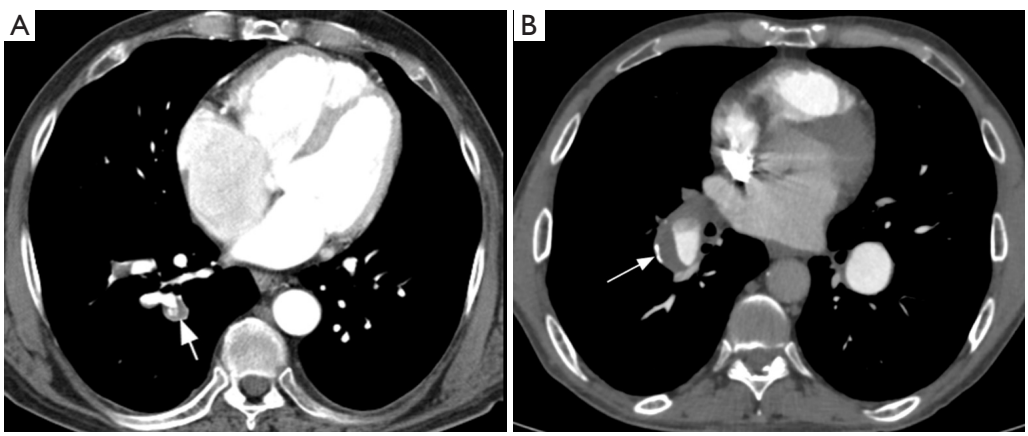

Figure 14 CT pulmonary angiography images in partially occlusive chronic pulmonary embolism. Note peripheral crescent-shaped defects presenting an obtuse angle with vessel wall (arrows in A and B) in contrast with acute angle observed in acute embolism (*Figure 13*).

Table 4 Differentiation of acute and chronic pulmonary thromboembolism—CT pulmonary angiography findings

CTPA findings	Acute	Chronic
Vascular signs	Central or eccentric filling defect; acute angle with vessel wall; preserved caliber of the artery or expanded secondary to pulsatile flow	Peripheral, crescent-shaped filling defect; obtuse angle with vessel wall; webs, bands, calcified thrombus; vessel narrowing or amputation, intimal irregularities
Collateral vessels	Absent	Bronchial and non-bronchial systemic arteries dilatation
Pulmonary hypertension signs	May be present; however, without right ventricle hypertrophy	Commonly present
Parenchymal signs	Pulmonary infarction ("reversed halo sign")	Pulmonary scars from prior infarction; mosaic lung attenuation

CTPA, computed tomography pulmonary angiography.

blindly at the hilum and the interruption of the artery is smooth without endoluminal changes (106). Blood supply of affected lung occurs through collateral systemic vessels, mainly bronchial arteries.

Takayasu arteritis

Takayasu arteritis is an idiopathic arteritis that mainly affects the aorta and its major branches. Pulmonary artery involvement may occur in 50–80% of patients and is usually a manifestation of late-stage disease. CT shows concentric inflammatory mural thickening of the arteries. Stenosis and occlusion mainly involve segmental and subsegmental arteries, affecting less commonly lobar or main pulmonary arteries. As in other chronic conditions of decreased pulmonary flow, collateral vessels may develop. The clue to the diagnosis of Takayasu arteritis versus CTEPH is presence of mural thickening and stenosis involving the aorta and its large branches (107).

Primary sarcoma of the pulmonary artery

Primary sarcoma of the pulmonary artery is a rare neoplasm. The types more frequently found are undifferentiated sarcoma and leiomyosarcoma. The main or proximal pulmonary arteries are most usually involved. The tumor manifests as an intraluminal filling defect on CT, resembling a thromboembolus. A filling defect occupying the entire arterial diameter is more common in primary pulmonary sarcoma than in thromboembolism. Extension of the lesion into the lung parenchyma or mediastinum and heterogeneous delayed enhancement at CT angiography are others signs that may help distinguishing between the two entities (108).

Idiopathic PAH

Clinically similar to CTEPH, idiopathic PAH may mimic CTEPH radiologically, particularly if *in situ* pulmonary artery thrombosis occurs as a complication of PAH. Some CT imaging findings frequently seen in CTEPH and hardly ever seen in idiopathic PAH are enlargement of bronchial and non-bronchial systemic arteries, mosaic lung attenuation, marked regional variation in the size of segmental vessels, and lung parenchymal scars (60,64,75).

Conclusions

Imaging plays a central role in the diagnosis of chronic PE and CTEPH, a condition frequently under or misdiagnosed, but potentially curable with surgery or endovascular intervention. Noninvasive techniques are complementary and not competing modalities in the investigation and management of CTEPH. Although V/Q scan is still considered the first line screening modality, CTPA has become an important piece in the diagnostic workup, capable of not only showing structural and vascular abnormalities, but also of ruling-out differential diagnoses. MRI provides functional and physiological data in a single modality, whereas other emerging methods such as SPECT/CT V/Q and DECT are also continually showing increments in diagnostic accuracy. In conclusion, the evolutions of all diagnostic modalities are responsible for continued improvement in the diagnosis of CTEPH, which in turn may result in more favorable patient outcomes.

Acknowledgements

None.

Footnote

Conflicts of Interest: The authors have no conflicts of interest to declare.

References

1. Beckman MG, Hooper WC, Critchley SE, et al. Venous thromboembolism: a public health concern. Am J Prev Med 2010;38:S495-501.
2. Pengo V, Lensing AW, Prins MH, et al. Incidence of chronic thromboembolic pulmonary hypertension after pulmonary embolism. N Engl J Med 2004;350:2257-64.
3. Ende-Verhaar YM, Cannegieter SC, Vonk Noordegraaf A, et al. Incidence of chronic thromboembolic pulmonary hypertension after acute pulmonary embolism: a contemporary view of the published literature. Eur Respir J 2017;49. pii: 1601792.
4. Lang IM, Pesavento R, Bonderman D, et al. Risk factors and basic mechanisms of chronic thromboembolic pulmonary hypertension: a current understanding. Eur Respir J 2013;41:462-8.
5. Humbert M. Pulmonary arterial hypertension and chronic thromboembolic pulmonary hypertension: pathophysiology. Eur Respir Rev 2010;19:59-63.
6. Simonneau G, Gatzoulis MA, Adatia I, et al. Updated clinical classification of pulmonary hypertension. J Am

Coll Cardiol 2013;62:D34-41.
7. Gall H, Hoeper MM, Richter MJ, et al. An epidemiological analysis of the burden of chronic thromboembolic pulmonary hypertension in the USA, Eur Respir Rev 2017;26. pii: 160121.
8. Strange G, Gabbay E, Kermeen F, et al. Time from symptoms to definitive diagnosis of idiopathic pulmonary arterial hypertension: The delay study. Pulm Circ 2013;3:89-94.
9. Lewczuk J, Piszko P, Jagas J, et al. Prognostic factors in medically treated patients with chronic pulmonary embolism. Chest 2001;119:818-23.
10. Galie N, Humbert M, Vachiery JL, et al. 2015 ESC/ERS Guidelines for the diagnosis and treatment of pulmonary hypertension: The Joint Task Force for the Diagnosis and Treatment of Pulmonary Hypertension of the European Society of Cardiology (ESC) and the European Respiratory Society (ERS): Endorsed by: Association for European Paediatric and Congenital Cardiology (AEPC), International Society for Heart and Lung Transplantation (ISHLT). Eur Respir J 2015;46:903-75.
11. Madani MM, Auger WR, Pretorius V, et al. Pulmonary endarterectomy: recent changes in a single institution's experience of more than 2,700 patients. Ann Thorac Surg 2012;94:97-103; discussion 103.
12. Corsico AG, D'Armini AM, Cerveri I, et al. Long-term outcome after pulmonary endarterectomy. Am J Respir Crit Care Med 2008;178:419-24.
13. Reesink HJ, Marcus JT, Tulevski II, et al. Reverse right ventricular remodeling after pulmonary endarterectomy in patients with chronic thromboembolic pulmonary hypertension: utility of magnetic resonance imaging to demonstrate restoration of the right ventricle. J Thorac Cardiovasc Surg 2007;133:58-64.
14. Iino M, Dymarkowski S, Chaothawee L, et al. Time course of reversed cardiac remodeling after pulmonary endarterectomy in patients with chronic pulmonary thromboembolism. Eur Radiol 2008;18:792-9.
15. Casaclang-Verzosa G, McCully RB, Oh JK, et al. Effects of pulmonary thromboendarterectomy on right-sided echocardiographic parameters in patients with chronic thromboembolic pulmonary hypertension. Mayo Clin Proc 2006;81:777-82.
16. Mizoguchi H, Ogawa A, Munemasa M, et al. Refined balloon pulmonary angioplasty for inoperable patients with chronic thromboembolic pulmonary hypertension. Circ Cardiovasc Interv 2012;5:748-55.
17. Fukui S, Ogo T, Morita Y, et al. Right ventricular reverse remodelling after balloon pulmonary angioplasty. Eur Respir J 2014;43:1394-402.
18. Fukui S, Ogo T, Goto Y, et al. Exercise intolerance and ventilatory inefficiency improve early after balloon pulmonary angioplasty in patients with inoperable chronic thromboembolic pulmonary hypertension. Int J Cardiol 2015;180:66-8.
19. Andreassen AK, Ragnarsson A, Gude E, et al. Balloon pulmonary angioplasty in patients with inoperable chronic thromboembolic pulmonary hypertension. Heart 2013;99:1415-20.
20. Yamasaki Y, Nagao M, Abe K, et al. Balloon pulmonary angioplasty improves interventricular dyssynchrony in patients with inoperable chronic thromboembolic pulmonary hypertension: a cardiac MR imaging study. Int J Cardiovasc Imaging 2017;33:229-39.
21. Blauwet LA, Edwards WD, Tazelaar HD, et al. Surgical pathology of pulmonary thromboendarterectomy: a study of 54 cases from 1990 to 2001. Hum Pathol 2003;34:1290-8.
22. Bonderman D, Wilkens H, Wakounig S, et al. Risk factors for chronic thromboembolic pulmonary hypertension. Eur Respir J 2009;33:325-31.
23. Simonneau G, Torbicki A, Dorfmuller P, et al. The pathophysiology of chronic thromboembolic pulmonary hypertension. Eur Respir Rev 2017;26. pii: 160112.
24. Yaoita N, Satoh K, Satoh T, et al. Thrombin-Activatable Fibrinolysis Inhibitor in Chronic Thromboembolic Pulmonary Hypertension. Arterioscler Thromb Vasc Biol 2016;36:1293-301.
25. Robbins IM, Pugh ME, Hemnes AR. Update on chronic thromboembolic pulmonary hypertension. Trends Cardiovasc Med 2017;27:29-37.
26. Fedullo PF, Auger WR, Kerr KM, et al. Chronic thromboembolic pulmonary hypertension. N Engl J Med 2001;345:1465-72.
27. Moser KM, Auger WR, Fedullo PF, et al. Chronic thromboembolic pulmonary hypertension: clinical picture and surgical treatment. Eur Respir J 1992;5:334-42.
28. Benza RL, Miller DP, Gomberg-Maitland M, et al. Predicting survival in pulmonary arterial hypertension: insights from the Registry to Evaluate Early and Long-Term Pulmonary Arterial Hypertension Disease Management (REVEAL). Circulation 2010;122:164-72.
29. Fritz JS, Blair C, Oudiz RJ, et al. Baseline and follow-up 6-min walk distance and brain natriuretic peptide predict 2-year mortality in pulmonary arterial hypertension. Chest 2013;143:315-23.

30. Expert Panel on Thoracic Imaging, Sirajuddin A, Donnelly EF, et al. ACR Appropriateness Criteria(R) Suspected Pulmonary Hypertension. J Am Coll Radiol 2017;14:S350-61.
31. Ghio S, Raineri C, Scelsi L, et al. Usefulness and limits of transthoracic echocardiography in the evaluation of patients with primary and chronic thromboembolic pulmonary hypertension. J Am Soc Echocardiogr 2002;15:1374-80.
32. Raisinghani A, Ben-Yehuda O. Echocardiography in chronic thromboembolic pulmonary hypertension. Semin Thorac Cardiovasc Surg 2006;18:230-5.
33. Woodruff WW 3rd, Hoeck BE, Chitwood WR Jr, et al. Radiographic findings in pulmonary hypertension from unresolved embolism. AJR Am J Roentgenol 1985;144:681-6.
34. Randall PA, Heitzman ER, Bull MJ, et al. Pulmonary arterial hypertension: a contemporary review. Radiographics 1989;9:905-27.
35. Satoh T, Kyotani S, Okano Y, et al. Descriptive patterns of severe chronic pulmonary hypertension by chest radiography. Respir Med 2005;99:329-36.
36. Tunariu N, Gibbs SJ, Win Z, et al. Ventilation-perfusion scintigraphy is more sensitive than multidetector CTPA in detecting chronic thromboembolic pulmonary disease as a treatable cause of pulmonary hypertension. J Nucl Med 2007;48:680-4.
37. He J, Fang W, Lv B, et al. Diagnosis of chronic thromboembolic pulmonary hypertension: comparison of ventilation/perfusion scanning and multidetector computed tomography pulmonary angiography with pulmonary angiography. Nucl Med Commun 2012;33:459-63.
38. Lisbona R, Kreisman H, Novales-Diaz J, et al. Perfusion lung scanning: differentiation of primary from thromboembolic pulmonary hypertension. AJR Am J Roentgenol 1985;144:27-30.
39. Powe JE, Palevsky HI, McCarthy KE, et al. Pulmonary arterial hypertension: value of perfusion scintigraphy. Radiology 1987;164:727-30.
40. Freeman LM. Don't bury the V/Q scan: it's as good as multidetector CT angiograms with a lot less radiation exposure. J Nucl Med 2008;49:5-8.
41. Meignan MA. Lung ventilation/perfusion SPECT: the right technique for hard times. J Nucl Med 2002;43:648-51.
42. Morrell NW, Nijran KS, Jones BE, et al. The underestimation of segmental defect size in radionuclide lung scanning. J Nucl Med 1993;34:370-4.
43. Morrell NW, Roberts CM, Jones BE, et al. The anatomy of radioisotope lung scanning. J Nucl Med 1992;33:676-83.
44. Ryan KL, Fedullo PF, Davis GB, et al. Perfusion scan findings understate the severity of angiographic and hemodynamic compromise in chronic thromboembolic pulmonary hypertension. Chest 1988;93:1180-5.
45. Collart JP, Roelants V, Vanpee D, et al. Is a lung perfusion scan obtained by using single photon emission computed tomography able to improve the radionuclide diagnosis of pulmonary embolism? Nucl Med Commun 2002;23:1107-13.
46. Soler X, Hoh CK, Test VJ, et al. Single photon emission computed tomography in chronic thromboembolic pulmonary hypertension. Respirology 2011;16:131-7.
47. Reinartz P, Wildberger JE, Schaefer W, et al. Tomographic imaging in the diagnosis of pulmonary embolism: a comparison between V/Q lung scintigraphy in SPECT technique and multislice spiral CT. J Nucl Med 2004;45:1501-8.
48. Soler X, Kerr KM, Marsh JJ, et al. Pilot study comparing SPECT perfusion scintigraphy with CT pulmonary angiography in chronic thromboembolic pulmonary hypertension. Respirology 2012;17:180-4.
49. Gutte H, Mortensen J, Jensen CV, et al. Detection of pulmonary embolism with combined ventilation-perfusion SPECT and low-dose CT: head-to-head comparison with multidetector CT angiography. J Nucl Med 2009;50:1987-92.
50. Expert Panels on Cardiac and Thoracic Imaging, Kirsch J, Brown RKJ, et al. ACR Appropriateness Criteria(R) Acute Chest Pain-Suspected Pulmonary Embolism. J Am Coll Radiol 2017;14:S2-12.
51. Ley S, Ley-Zaporozhan J, Pitton MB, et al. Diagnostic performance of state-of-the-art imaging techniques for morphological assessment of vascular abnormalities in patients with chronic thromboembolic pulmonary hypertension (CTEPH). Eur Radiol 2012;22:607-16.
52. Reichelt A, Hoeper MM, Galanski M, et al. Chronic thromboembolic pulmonary hypertension: evaluation with 64-detector row CT versus digital substraction angiography. Eur J Radiol 2009;71:49-54.
53. Sugiura T, Tanabe N, Matsuura Y, et al. Role of 320-slice CT imaging in the diagnostic workup of patients with chronic thromboembolic pulmonary hypertension. Chest 2013;143:1070-7.
54. Mettler FA, Huda W, Yoshizumi TT, et al. Effective doses in radiology and diagnostic nuclear medicine: a catalog. Radiology 2008;248:254-63.

55. Schembri GP, Miller AE, Smart R. Radiation dosimetry and safety issues in the investigation of pulmonary embolism. Semin Nucl Med 2010;40:442-54.
56. Heyer CM, Mohr PS, Lemburg SP, et al. Image quality and radiation exposure at pulmonary CT angiography with 100- or 120-kVp protocol: prospective randomized study. Radiology 2007;245:577-83.
57. Gill MK, Vijayananthan A, Kumar G, et al. Use of 100 kV versus 120 kV in computed tomography pulmonary angiography in the detection of pulmonary embolism: effect on radiation dose and image quality. Quant Imaging Med Surg 2015;5:524-33.
58. Szucs-Farkas Z, Kurmann L, Strautz T, et al. Patient exposure and image quality of low-dose pulmonary computed tomography angiography: comparison of 100- and 80-kVp protocols. Invest Radiol 2008;43:871-6.
59. Sauter A, Koehler T, Fingerle AA, et al. Ultra Low Dose CT Pulmonary Angiography with Iterative Reconstruction. PLoS One 2016;11:e0162716.
60. King MA, Ysrael M, Bergin CJ. Chronic thromboembolic pulmonary hypertension: CT findings. AJR Am J Roentgenol 1998;170:955-60.
61. Renapurkar RD, Shrikanthan S, Heresi GA, et al. Imaging in Chronic Thromboembolic Pulmonary Hypertension. J Thorac Imaging 2017;32:71-88.
62. Korn D, Gore I, Blenke A, et al. Pulmonary arterial bands and webs: an unrecognized manifestation of organized pulmonary emboli. Am J Pathol 1962;40:129-51.
63. Kauczor HU, Schwickert HC, Mayer E, et al. Spiral CT of bronchial arteries in chronic thromboembolism. J Comput Assist Tomogr 1994;18:855-61.
64. Remy-Jardin M, Duhamel A, Deken V, et al. Systemic collateral supply in patients with chronic thromboembolic and primary pulmonary hypertension: assessment with multi-detector row helical CT angiography. Radiology 2005;235:274-81.
65. Tan RT, Kuzo R, Goodman LR, et al. Utility of CT scan evaluation for predicting pulmonary hypertension in patients with parenchymal lung disease. Medical College of Wisconsin Lung Transplant Group. Chest 1998;113:1250-6.
66. Ng CS, Wells AU, Padley SP. A CT sign of chronic pulmonary arterial hypertension: the ratio of main pulmonary artery to aortic diameter. J Thorac Imaging 1999;14:270-8.
67. Raymond TE, Khabbaza JE, Yadav R, et al. Significance of main pulmonary artery dilation on imaging studies. Ann Am Thorac Soc 2014;11:1623-32.
68. Quiroz R, Kucher N, Schoepf UJ, et al. Right ventricular enlargement on chest computed tomography: prognostic role in acute pulmonary embolism. Circulation 2004;109:2401-4.
69. Schoepf UJ, Kucher N, Kipfmueller F, et al. Right ventricular enlargement on chest computed tomography: a predictor of early death in acute pulmonary embolism. Circulation 2004;110:3276-80.
70. van der Meer RW, Pattynama PM, van Strijen MJ, et al. Right ventricular dysfunction and pulmonary obstruction index at helical CT: prediction of clinical outcome during 3-month follow-up in patients with acute pulmonary embolism. Radiology 2005;235:798-803.
71. Oliver TB, Reid JH, Murchison JT. Interventricular septal shift due to massive pulmonary embolism shown by CT pulmonary angiography: an old sign revisited. Thorax 1998;53:1092-4; discussion 1088-9.
72. King MA, Bergin CJ, Yeung DW, et al. Chronic pulmonary thromboembolism: detection of regional hypoperfusion with CT. Radiology 1994;191:359-63.
73. Bergin CJ, Sirlin C, Deutsch R, et al. Predictors of patient response to pulmonary thromboendarterectomy. AJR Am J Roentgenol 2000;174:509-15.
74. Bergin CJ, Rios G, King MA, et al. Accuracy of high-resolution CT in identifying chronic pulmonary thromboembolic disease. AJR Am J Roentgenol 1996;166:1371-7.
75. Sherrick AD, Swensen SJ, Hartman TE. Mosaic pattern of lung attenuation on CT scans: frequency among patients with pulmonary artery hypertension of different causes. AJR Am J Roentgenol 1997;169:79-82.
76. Arakawa H, Stern EJ, Nakamoto T, et al. Chronic pulmonary thromboembolism. Air trapping on computed tomography and correlation with pulmonary function tests. J Comput Assist Tomogr 2003;27:735-42.
77. Arakawa H, Kurihara Y, Sasaka K, et al. Air trapping on CT of patients with pulmonary embolism. AJR Am J Roentgenol 2002;178:1201-7.
78. Auger WR, Fedullo PF, Moser KM, et al. Chronic major-vessel thromboembolic pulmonary artery obstruction: appearance at angiography. Radiology 1992;182:393-8.
79. Pepke-Zaba J, Delcroix M, Lang I, et al. Chronic thromboembolic pulmonary hypertension (CTEPH): results from an international prospective registry. Circulation 2011;124:1973-81.
80. Hoeper MM, Mayer E, Simonneau G, et al. Chronic thromboembolic pulmonary hypertension. Circulation 2006;113:2011-20.

81. McCollough CH, Leng S, Yu L, et al. Dual- and Multi-Energy CT: Principles, Technical Approaches, and Clinical Applications. Radiology 2015;276:637-53.
82. Fuld MK, Halaweish AF, Haynes SE, et al. Pulmonary perfused blood volume with dual-energy CT as surrogate for pulmonary perfusion assessed with dynamic multidetector CT. Radiology 2013;267:747-56.
83. Thieme SF, Becker CR, Hacker M, et al. Dual energy CT for the assessment of lung perfusion--correlation to scintigraphy. Eur J Radiol 2008;68:369-74.
84. Thieme SF, Johnson TR, Lee C, et al. Dual-energy CT for the assessment of contrast material distribution in the pulmonary parenchyma. AJR Am J Roentgenol 2009;193:144-9.
85. Thieme SF, Graute V, Nikolaou K, et al. Dual Energy CT lung perfusion imaging--correlation with SPECT/CT. Eur J Radiol 2012;81:360-5.
86. Boroto K, Remy-Jardin M, Flohr T, et al. Thoracic applications of dual-source CT technology. Eur J Radiol 2008;68:375-84.
87. Ko JP, Brandman S, Stember J, et al. Dual-energy computed tomography: concepts, performance, and thoracic applications. J Thorac Imaging 2012;27:7-22.
88. Ameli-Renani S, Rahman F, Nair A, et al. Dual-energy CT for imaging of pulmonary hypertension: challenges and opportunities. Radiographics 2014;34:1769-90.
89. Kang MJ, Park CM, Lee CH, et al. Focal iodine defects on color-coded iodine perfusion maps of dual-energy pulmonary CT angiography images: a potential diagnostic pitfall. AJR Am J Roentgenol 2010;195:W325-30.
90. Ferda J, Ferdova E, Mirka H, et al. Pulmonary imaging using dual-energy CT, a role of the assessment of iodine and air distribution. Eur J Radiol 2011;77:287-93.
91. Renard B, Remy-Jardin M, Santangelo T, et al. Dual-energy CT angiography of chronic thromboembolic disease: can it help recognize links between the severity of pulmonary arterial obstruction and perfusion defects? Eur J Radiol 2011;79:467-72.
92. Nakazawa T, Watanabe Y, Hori Y, et al. Lung perfused blood volume images with dual-energy computed tomography for chronic thromboembolic pulmonary hypertension: correlation to scintigraphy with single-photon emission computed tomography. J Comput Assist Tomogr 2011;35:590-5.
93. Dournes G, Verdier D, Montaudon M, et al. Dual-energy CT perfusion and angiography in chronic thromboembolic pulmonary hypertension: diagnostic accuracy and concordance with radionuclide scintigraphy. Eur Radiol 2014;24:42-51.
94. Meinel FG, Graef A, Thierfelder KM, et al. Automated quantification of pulmonary perfused blood volume by dual-energy CTPA in chronic thromboembolic pulmonary hypertension. Rofo 2014;186:151-6.
95. Ameli-Renani S, Ramsay L, Bacon JL, et al. Dual-energy computed tomography in the assessment of vascular and parenchymal enhancement in suspected pulmonary hypertension. J Thorac Imaging 2014;29:98-106.
96. Kreitner KF, Ley S, Kauczor HU, et al. Chronic thromboembolic pulmonary hypertension: pre- and postoperative assessment with breath-hold MR imaging techniques. Radiology 2004;232:535-43.
97. Rajaram S, Swift AJ, Telfer A, et al. 3D contrast-enhanced lung perfusion MRI is an effective screening tool for chronic thromboembolic pulmonary hypertension: results from the ASPIRE Registry. Thorax 2013;68:677-8.
98. Ley S, Kramm T, Kauczor HU, et al. Pre- and postoperative assessment of hemodynamics in patients with chronic thromboembolic pulmonary hypertension by MR techniques. Rofo 2003;175:1647-54.
99. Zhang B, Liang L, Chen W, et al. An Updated Study to Determine Association between Gadolinium-Based Contrast Agents and Nephrogenic Systemic Fibrosis. PLoS One 2015;10:e0129720.
100. ACR Committee on Drugs and Contrast Media. Manual on Contrast Media v10.3. 2017. Available online: https://www.acr.org/Quality-Safety/Resources/Contrast-Manual. Accessed 11/30/2017.
101. Kanda T, Nakai Y, Hagiwara A, et al. Distribution and chemical forms of gadolinium in the brain: a review. Br J Radiol 2017;90:20170115.
102. FDA. FDA Drug Safety Communication: FDA identifies no harmful effects to date with brain retention of gadolinium-based contrast agents for MRIs; review to continue. 2017. Available online: https://www.fda.gov/Drugs/DrugSafety/ucm559007.htm. Accessed 11/30/2017.
103. Remy-Jardin M, Remy J, Wattinne L, et al. Central pulmonary thromboembolism: diagnosis with spiral volumetric CT with the single-breath-hold technique--comparison with pulmonary angiography. Radiology 1992;185:381-7.
104. Castañer E, Gallardo X, Ballesteros E, et al. CT diagnosis of chronic pulmonary thromboembolism. Radiographics 2009;29:31-50; discussion 50-3.
105. Ruggiero A, Screaton NJ. Imaging of acute and chronic thromboembolic disease: state of the art. Clin Radiol

2017;72:375-88.
106. Ten Harkel AD, Blom NA, Ottenkamp J. Isolated unilateral absence of a pulmonary artery: a case report and review of the literature. Chest 2002;122:1471-7.
107. Matsunaga N, Hayashi K, Sakamoto I, et al. Takayasu arteritis: protean radiologic manifestations and diagnosis. Radiographics 1997;17:579-94.
108. Yi CA, Lee KS, Choe YH, et al. Computed tomography in pulmonary artery sarcoma: distinguishing features from pulmonary embolic disease. J Comput Assist Tomogr 2004;28:34-9.

Cite this article as: Nishiyama KH, Saboo SS, Tanabe Y, Jasinowodolinski D, Landay MJ, Kay FU. Chronic pulmonary embolism: diagnosis. Cardiovasc Diagn Ther 2018;8(3):253-271. doi: 10.21037/cdt.2018.01.09

